Coherences and populations in the driven damped two-state system

Milena Grifoni,[1] Manfred Winterstetter,[2] and Ulrich Weiss[2]
[1]*Institut für Physik, Universität Augsburg, Memminger Straβe 6, D-86135 Augsburg, Germany*
[2]*Institut für Theoretische Physik, Universität Stuttgart, Pfaffenwaldring 57, D-70550 Stuttgart, Germany*
(Received 27 February 1997)

The dynamics of the density matrix of the two-state system under the influence of time-dependent deterministic and fluctuating forces is investigated. The exact formal solutions for the diagonal and off-diagonal elements are derived and transformed into coupled nonconvolutive master equations and integral relations. Thereby, the evolution of *any* observable relevant to the two-state system may be described. Solutions of the dynamical equations in analytic form are presented both for high and low temperatures. An iterative numerical method is put forward in which the familiar noninteracting-blip approximation is systematically improved by taking into account all bath-induced nearest-neighbor interblip correlations. The expanded treatment is found to be indispensable in studies of the dynamics of the off-diagonal elements at low temperatures. Finally, we discuss selection rules, as well as possibilities of control of tunneling, which occur in the presence of monochromatic driving. [S1063-651X(97)11007-8]

PACS number(s): 05.30.−d, 05.40.+j, 33.80.Be

I. INTRODUCTION

The model of a quantum particle moving in a double well potential and being in contact with a heat bath environment has widespread application in diverse physical and chemical systems. It has been used, e.g., to describe long range electron-transfer reactions [1], the tunneling of atoms between an atomic-force microscope tip and a surface [2], or the magnetic flux dynamics in a superconducting quantum interference device [3]. At sufficiently low temperatures, the system can be effectively restricted to the two-dimensional Hilbert space spanned by the ground states of the two potential minima. Complete information on the damped tunneling dynamics of this two-state system (TSS) is contained in the reduced density matrix (RDM) of the system. In the basis representation of the localized states, the diagonal elements represent the *populations*. In contrast, the off-diagonal elements of the RDM, the so-called ''coherences,'' describe quantum interference effects. In the recent past, lots of efforts have been dedicated to the evaluation of the populations [4–6].

The isolated TSS is the simplest system exhibiting quantum interference effects. Namely, it may be prepared such that it exhibits clockwise oscillations of the populations of the two localized states. The influence of a stochastic force generally results in a reduction of the coherent motion and may lead to pure monotonous relaxation towards the equilibrium state for sufficiently high temperature and/or damping. It may even lead to a transition to localization at zero temperature [7]. Besides the stochastic force, the system may be influenced by a deterministic time-dependent force. There have been made numerous studies about the control of tunneling by time-dependent external fields [8–19].

In this work, we concentrate the discussion on the off-diagonal elements of the RDM. The coherences have been studied recently within the traditional optical Bloch equations by employing the weak-damping limit and by treating the propelling field in the rotating-wave approximation [20]. Here we present the exact formal solution for the RDM and we give exact relations between the matrix elements. As a result of the analysis, we can then describe the time evolution of the mean value of *any* observable relevant to the TSS. As an example, we study, both analytically and numerically, the time evolution of the real and of the imaginary part of the coherences.

This paper is structured as follows. In Sec. II, we introduce the model and the relevant dynamical quantities. In Sec. III A, we derive the exact formal solution for the populations and coherences. The related set of closed dynamical equations is given in Sec. III B. In Sec. IV, we present results of the system's dynamics in analytic form in various limits. The noninteracting-blip approximation (NIBA) for the stochastic forces is briefly considered in Sec. IV A. The dynamics in the Markov limit and for a static bias is presented in Sec. IV B. The dynamics for weak damping and low temperatures is discussed in Sec. IV C. For a static bias, the corrections beyond the NIBA are presented in analytic form. In Sec. V, we describe a treatment of the random force beyond the NIBA which we refer to as the ''interacting-blip chain approximation'' (IBCA) [21]. In the IBCA, the bath-induced correlations within all nearest-neighbor blip-sojourn-blip intervals are fully taken into account. In Sec. VI, the various methods are applied and numerically evaluated in some regimes. The conclusions are drawn in Sec. VII.

II. THE DRIVEN DAMPED SYSTEM

Tunneling phenomena in physics and chemistry can often be modeled by a dissipative particle with only few accessible localized states. As a working model, we consider the case of two states, and damping comes about through contact with a heat bath, which is represented by an ensemble of linearly responding oscillator modes with a continuum of eigenfrequencies. This is the familiar spin-boson model [4–6], and its usefulness in describing transfer dynamics in condensed phases has been well established. To be general, we allow for time-dependent modulation of both the transfer matrix element Δ and the biasing energy ε. The Hamiltonian of the

TSS alone may be written in the form (we put $\hbar = k_B = 1$)

$$H(t) = -\Delta(t)\sigma_x/2 - [\varepsilon(t) + \zeta(t)]\sigma_z/2. \tag{2.1}$$

Here, the σ's are Pauli matrices, and the basis states are the localized eigenstates $|R\rangle$ (right) and $|L\rangle$ (left) of σ_z with eigenvalues $+1$ and -1, respectively. We then have $\sigma_x = |L\rangle\langle R| + |R\rangle\langle L|$ and $\sigma_z = |R\rangle\langle R| - |L\rangle\langle L|$.

The variation of Δ with time arises from a modulation of the barrier of the underlying double well potential. For harmonic barrier drive, we have $\Delta(t) = \Delta_0 \exp(\mu \cos\Omega t)$, where μ is a suitable dimensionless amplitude (see the discussion in Ref. [19]). The quantity $\varepsilon(t)$ is the deterministic bias energy. It is conveniently decomposed as

$$\varepsilon(t) = \epsilon_0 + f(t), \tag{2.2}$$

where ϵ_0 is a bias related to intrinsic static strains, and $f(t)$ is a bias modulation due to an externally applied time-dependent force. For electron transfer in a solvent, we conceive of controlling charge tunneling by application of strong continuous laser fields. Regarding charge transfer in nanostructures, we think of regulating the dynamics by turning on microwave irradiation or a high-frequency voltage. In pump-probe setups, the driving force is pulse shaped.

The coupling to a heat bath or solvent is captured by a fluctuating force $\zeta(t)$. For a linear-response reservoir at fixed temperature T, $\zeta(t)$ obeys stationary Gaussian statistics. It is fully characterized by $\langle \zeta(t) \rangle_T = 0$ and by the force autocorrelation function [4,6]

$$\langle \zeta(t)\zeta(0) \rangle_T = \frac{1}{\pi} \int_0^\infty d\omega J(\omega) \frac{\cosh(\omega/2T - i\omega t)}{\sinh(\omega/2T)}. \tag{2.3}$$

As long as we are interested in the reduced dynamics of the TSS alone (RDM), all effects of the environment are completely specified by the spectral density $J(\omega)$. An important case is the Ohmic form

$$J(\omega) = 2\pi\alpha\omega \exp(-\omega/\omega_c), \tag{2.4}$$

which is employed in the numerical simulations reported below. Ohmic damping is of widespread importance in physical and chemical condensed phase reactions [4–6]. The dimensionless friction parameter α measures the strength of frequency-independent damping, and ω_c is a high-frequency cutoff for the bath modes. Most of the subsequent expressions, however, are valid for general frequency-dependent linear dissipation. Similarly, the numerical IBCA method presented below is also not limited to the case of Ohmic damping.

The RDM is a 2×2 matrix with diagonal elements $\rho_{-1,-1}$ and $\rho_{1,1}$, and off-diagonal elements (coherences) $\rho_{-1,1}$ and $\rho_{1,-1}$. It can be written as a linear combination of the Pauli matrices and of the unit matrix I, $\rho(t) = I/2 + \Sigma_{i=x,y,z} \langle \sigma_i \rangle_t \sigma_i/2$, where $\langle \sigma_i \rangle_t \equiv \langle R | \langle \sigma_i(t) \rangle_T | R \rangle$. Here $\langle \cdots \rangle_T$ denotes thermal average according to Eq. (2.3), and $\langle R | \cdots | R \rangle$ is the expectation value with respect to the initial state $|R\rangle (\equiv |1\rangle)$ of the TSS. *Any* mean value may be expressed in terms of $\rho(t)$,

$$\langle \sigma_z \rangle_t = \rho_{1,1}(t) - \rho_{-1,-1}(t), \tag{2.5}$$

$$\langle \sigma_x \rangle_t = \rho_{1,-1}(t) + \rho_{-1,1}(t),$$

$$\langle \sigma_y \rangle_t = i[\rho_{1,-1}(t) - \rho_{-1,1}(t)].$$

According to the chosen initial condition, we have $\rho_{\sigma,\sigma'}(t=0) = \delta_{\sigma,1}\delta_{\sigma',1}$. The quantity $\langle \sigma_z \rangle_t$ describes the difference of the populations of the two localized states. It gives direct information about the tunneling dynamics. The understanding of the TSS dynamics is completed by the knowledge of the coherences $\langle \sigma_x \rangle_t$ and $\langle \sigma_y \rangle_t$.

In the absence of driving and dissipation, the RDM can be evaluated straightforwardly, yielding

$$\langle \sigma_z \rangle_t = \epsilon_0^2/E^2 + (\Delta^2/E^2)\cos(Et),$$

$$\langle \sigma_x \rangle_t = (\epsilon_0\Delta/E^2)[1 - \cos(Et)], \tag{2.6}$$

$$\langle \sigma_y \rangle_t = (\Delta/E)\sin(Et).$$

As a result of quantum interference, the RDM shows undamped oscillations with frequency $E = (\Delta^2 + \epsilon_0^2)^{1/2}$, which is the level splitting of the isolated TSS. For the symmetric TSS ($\epsilon_0 = 0$), the eigenstates of σ_x are just those of the isolated TSS Hamiltonian. Consequently, the initial value $\langle \sigma_x \rangle_{t=0} = 0$ is kept for all $t > 0$.

In the following sections, we study the evolution of the expectation values (2.5) of the RDM in the presence of driving and dissipation.

III. THE REDUCED DENSITY MATRIX

A. The exact formal solution

The reduced density matrix $\rho_{\sigma,\sigma'}(t)$ is conveniently expressed in terms of a real-time double path integral,

$$\rho_{\sigma,\sigma'}(t) = \int \mathcal{D}q \int \mathcal{D}q' \, \mathcal{A}[q]\mathcal{B}[q]\mathcal{A}^*[q']\mathcal{B}^*[q'] e^{-\Phi[q,q']}.$$

For initial state $\rho_{\sigma,\sigma'}(0) = \delta_{\sigma,1}\delta_{\sigma',1}$, the path sum is over all spin paths $q(t'), q'(t')$ with boundary conditions $q(0) = q'(0) = 1/2, q(t) = \sigma/2$, and $q'(t) = \sigma'/2$. For a TSS, the paths $q(t')$ and $q'(t')$ jump back and forth between the positions $+1/2$ and $-1/2$. The quantity $\mathcal{A}[q]$ is the probability amplitude of the TSS to follow the path $q(t')$ in the absence of biasing and fluctuating forces. The deterministic biasing forces are encapsulated in the factor

$$\mathcal{B}[q] = \exp\left\{ i \int_0^t dt' [\epsilon_0 + f(t')] q(t') \right\}. \tag{3.1}$$

The influence function $\Phi[q,q']$ captures the influences of the fluctuating force $\zeta(t)$. For Gaussian statistics [6,22],

$$\Phi = \int_0^t dt' \int_0^{t'} dt'' [q(t') - q'(t')][\langle \zeta(t')\zeta(t'') \rangle_T q(t'') - \langle \zeta(t'')\zeta(t') \rangle_T q'(t'')].$$

Finally, $\int \mathcal{D}q$ symbolically means summation in function space over all paths with fixed boundaries. In studies of the dynamics of the RDM, it is convenient to introduce the symmetric and antisymmetric spin paths ($0 \leqslant \tau \leqslant t$):

$$\eta(\tau)=q(\tau)+q'(\tau), \quad \xi(\tau)=q(\tau)-q'(\tau).$$

The path $\eta(\tau)$ describes propagation straight along the diagonal of the density matrix and can therefore be identified with the quasiclassical path. On the other hand, the path $\xi(\tau)$ records the off-diagonal excursions and therefore is connected with the quantum fluctuations. An interval during which the system propagates in an off-diagonal state is termed *blip* while an interval with propagation in a diagonal state is called *sojourn*. During a sojourn, the function $\xi(\tau)$ is zero, while during a blip interval, the function $\eta(\tau)$ is zero. There are two sojourn and two blip states labeled by $\eta=\pm 1$ and $\xi=\pm 1$, respectively. For the two-state system, the paths $\eta(\tau)$ and $\xi(\tau)$ undergo sudden transitions between blip states $\{\xi_j\}$ and sojourn states $\{\eta_k\}$ and vice versa at flip times $\{t_i\}$.

Consider now a definite path making a total of $2n$ transitions that starts in the state $\eta_0=+1$ and ends in the state $\eta_n=f(=\pm 1)$. Assume that the flip times are chronologically ordered, $0\leqslant t_1\leqslant\cdots\leqslant t_{2n}\leqslant t$. The path consists of n blips and $n+1$ sojourns, where $s_j=t_{2j+1}-t_{2j}$ and $\tau_j=t_{2j}-t_{2j-1}$ are the sojourn and blip lengths, respectively. The auxiliary flip times t_0 and t_{2n+1} are displaced to the infinite past and future.

As the paths are piecewise constant, the influence function Φ is conveniently expressed in terms of the second integral of the force correlation function (2.3),

$$Q(\tau)=\frac{1}{\pi}\int_0^\infty d\omega\,\frac{J(\omega)}{\omega^2}\,\frac{\cosh(\omega/2T)-\cosh(\omega/2T-i\omega\tau)}{\sinh(\omega/2T)}.$$

For a path with n blips and $n+1$ sojourns, we have

$$\Phi^{(n)}=\sum_{j=1}^{n}\left[S_j-i\sum_{k=0}^{j-1}\xi_j\eta_k X_{j,k}\right]+\sum_{j=2}^{n}\sum_{k=1}^{j-1}\xi_j\xi_k\Lambda_{j,k}.$$

The interactions S_j $(j=1,\ldots,n)$ are the blip self-interactions (intrablip interactions). The function $\Lambda_{j,k}$ with $j\neq k$ represents the interactions between the blip pair $\{j,k\}$, and the term $X_{j,k}$ describes the interactions between the blip j and the earlier sojourn k. Upon introducing the notations $Q_{j,k}=Q(t_j-t_k)$ and $Q(\tau)=Q'(\tau)+iQ''(\tau)$, the interactions read

$$S_j=Q'_{2j,2j-1}=Q'(\tau_j),$$

$$\Lambda_{j,k}=Q'_{2j,2k-1}+Q'_{2j-1,2k}-Q'_{2j,2k}-Q'_{2j-1,2k-1},$$

$$X_{j,k}=Q''_{2j,2k+1}+Q''_{2j-1,2k}-Q''_{2j,2k}-Q''_{2j-1,2k+1}.$$

The summation over the history of paths contributing to $\langle\sigma_i\rangle_t$ $(i=z,x,y)$ results in an expansion in the number of tunneling transitions. The number is even for $\langle\sigma_z\rangle_t$, while it is odd for $\langle\sigma_x\rangle_t$ and $\langle\sigma_y\rangle_t$. The integration over the flip times is compactly expressed by the notation

$$\int_{t_0}^{t}\mathcal{D}_n\{t_j\}\cdots\equiv\int_{t_0}^{t}dt_n\int_{t_0}^{t_n}dt_{n-1}\cdots\int_{t_0}^{t_2}dt_1\cdots. \quad (3.2)$$

Before turning to the discussion of $\langle\sigma_x\rangle_t$ and $\langle\sigma_y\rangle_t$, we briefly summarize previous findings on the quantity $\langle\sigma_z\rangle_t$ [10,13,14,19]. With the appropriate generalization to the present model, the exact formal solution for $\langle\sigma_z\rangle_t$ is

$$\langle\sigma_z\rangle_t=1+\sum_{n=1}^{\infty}(-1)^n\int_0^t\mathcal{D}_{2n}\{t_j\}\Delta_{2n}(\{t_j\})2^{-n}$$

$$\times\sum_{\{\xi_j=\pm 1\}}(F_n^{(+)}C_n^{(+)}-F_n^{(-)}C_n^{(-)}). \quad (3.3)$$

Here, $\Delta_m(\{t_j\})$ is the product of m (bare) probability amplitudes for tunneling at the set of flip times $\{t_j\}$,

$$\Delta_m(\{t_j\})=\prod_{j=1}^{m}\Delta(t_j).$$

The influences of the stochastic force are in the functions $F_n^{(\pm)}$, while the effects of the deterministic force are encapsulated in the factors $C_n^{(\pm)}$ given below. In the expression (3.3), the summation over the intermediate sojourn states has been performed already. The remaining ξ summation represents the 2^n possibilities of arranging n blips. Next, we turn to the discussion of the off-diagonal elements. Since now the final hop back to the diagonal is missing, all paths dwell at time t in the final blip state, i.e., $\xi(t)=1$ or -1, depending on whether one considers the state $\rho_{1,-1}(t)$ or $\rho_{-1,1}(t)$. Upon employing Eq. (2.5), the exact formal expressions for the off diagonal linear combinations $\langle\sigma_x\rangle_t$ and $\langle\sigma_y\rangle_t$ are found to read

$$\langle\sigma_x\rangle_t=\sum_{n=1}^{\infty}(-1)^{n-1}\int_0^t\mathcal{D}_{2n-1}\{t_j\}\Delta_{2n-1}(\{t_j\})2^{-n}$$

$$\times\sum_{\{\xi_j=\pm 1\}}\xi_n(F_n^{(+)}C_n^{(-)}+F_n^{(-)}C_n^{(+)}), \quad (3.4)$$

$$\langle\sigma_y\rangle_t=\sum_{n=1}^{\infty}(-1)^{n-1}\int_0^t\mathcal{D}_{2n-1}\{t_j\}\Delta_{2n-1}(\{t_j\})2^{-n}$$

$$\times\sum_{\{\xi_j=\pm 1\}}(F_n^{(+)}C_n^{(+)}-F_n^{(-)}C_n^{(-)}). \quad (3.5)$$

The biasing forces lead to phase factors

$$C_n^{(+)}=\cos\varphi_n, \quad C_n^{(-)}=\sin\varphi_n, \quad (3.6)$$

where $\varphi_n=\Sigma_{j=1}^{n}\xi_j\vartheta(t_{2j},t_{2j-1})$ is the phase accumulated from the n blips, and $\xi_j\vartheta(t_{2j},t_{2j-1})$ is the phase from blip j of type ξ_j, where

$$\vartheta(t_{2j},t_{2j-1})=\int_{t_{2j-1}}^{t_{2j}}dt'\varepsilon(t'). \quad (3.7)$$

In order to represent the influence factors $F_n^{(\pm)}$ in compact form, we combine the intrablip and interblip correlations of n blips in the expression

$$G_n=\exp\left(-\sum_{j=1}^{n}Q'_{2j,2j-1}-\sum_{j=2}^{n}\sum_{k=1}^{j-1}\xi_j\xi_k\Lambda_{j,k}\right),$$

and we introduce the phases $\chi_{n,k}=\Sigma_{j=k+1}^{n}\xi_j X_{j,k}$. They describe the bath correlations between the sojourn k and the $n-k$ succeeding blips. Then, the full influence functions $F_n^{(\pm)}$ take the form

$$F_n^{(+)}=G_n\prod_{k=0}^{n-1}\cos\chi_{n,k},\quad F_n^{(-)}=F_n^{(+)}\tan\chi_{n,0}. \tag{3.8}$$

For the Ohmic spectral density (2.4), $Q(\tau)$ reads [24]

$$Q'(\tau)=2\alpha\ln\left(\frac{\Gamma^2(\kappa)\sqrt{1+\omega_c^2\tau^2}}{\Gamma(\kappa+iT\tau)\Gamma(\kappa-iT\tau)}\right),$$

$$Q''(\tau)=2\alpha\arctan(\omega_c\tau), \tag{3.9}$$

where $\Gamma(z)$ is the gamma function, and $\kappa=1+T/\omega_c$. This form holds for arbitrary cutoff frequency ω_c. It is employed in the numerical simulations reported below.

Analytical studies are made easier in the limit of large ω_c, in which Eq. (3.9) reduces to the more familiar form

$$Q'(\tau)=2\alpha\ln[(\omega_c/\pi T)\sinh(\pi T\tau)],$$

$$Q''(\tau)=\pi\alpha\,\mathrm{sgn}(\tau). \tag{3.10}$$

The exact formal series expressions (3.3), (3.4), and (3.5) are rather intricate, and they are by far too complicated to be handled analytically. Hence, one has to resort to suitable approximations. Before proceeding along these lines, it is advantageous to cast the expression for $\langle\sigma_z\rangle_t$ into the form of a master equation and the expression for $\langle\sigma_x\rangle_t$ into an integral relation. Interestingly, this proceeding can be performed exactly.

B. Exact master equation and integral relation

In previous work, it has been shown that the exact formal series expression (3.3) for $\langle\sigma_z\rangle_t$ can be rewritten in the form of a generalized master equation (GME) [14],

$$\frac{d\langle\sigma_z\rangle_t}{dt}=\int_0^t dt'[K_z^{(-)}(t,t')-K_z^{(+)}(t,t')\langle\sigma_z\rangle_{t'}]. \tag{3.11}$$

The upper labels $(+)$ and $(-)$ indicate whether the kernel is an even or odd function of the bias. The kernels themselves are defined in terms of the series expressions

$$K_z^{(\pm)}(t,t')=\sum_{n=1}^{\infty}(-1)^{n-1}\int_{t'}^{t}dt_{2n-1}\cdots \times\int_{t'}^{t_3}dt_2\Delta_{2n}(\{t_j\})2^{-n}\sum_{\{\xi_j=\pm1\}}\widetilde{F}_n^{(\pm)}C_n^{(\pm)}. \tag{3.12}$$

The product functions $\widetilde{F}_n^{(\pm)}C_n^{(\pm)}$ depend on $2n$ flip times. The first one and the last one are identified by t' and with t. The $2n-2$ intermediate flip times are integrated out.

It is now important that the functions $\widetilde{F}_n^{(\pm)}$ are modified influence functions involving suitable subtractions of products of lower order influence functions. This is because the iteration of the GME produces products of uncorrelated influence functions that are absent in the original expression (3.3). For instance, in the third step of the iteration of Eq. (3.11) there appear terms $\widetilde{F}_{n_1}^{(+)}\widetilde{F}_{n_2}^{(+)}\widetilde{F}_{n_3}^{(\pm)}$, where n_1,n_2,n_3 are arbitrary positive integers. The modified influence function $\widetilde{F}_n^{(\pm)}$ is now defined in such a way that these unwanted terms cancel each other. The analysis yields that the influence functions $\widetilde{F}_n^{(\pm)}$ are defined in terms of the original influence functions $F_n^{(\pm)}$ by

$$\widetilde{F}_n^{(\pm)}=F_n^{(\pm)}-\sum_{j=2}^{n}(-1)^j\sum_{m_1,\cdots,m_j}F_{m_1}^{(+)}F_{m_2}^{(+)}\cdots \times F_{m_j}^{(\pm)}\delta_{m_1+\cdots+m_j,n}.$$

The inner sum is over positive integers m_j. By definition, each subtraction involves again time ordering of the flip times, with t_1 being the earliest. In the subtracted terms, the bath correlations are only inside of the individual factors $F_{m_j}^{(\pm)}$. Correlations between these factors are absent.

It is interesting to note that the quantity $\langle\sigma_x\rangle_t$ is connected with $\langle\sigma_z\rangle_t$ by the exact integral relation

$$\langle\sigma_x\rangle_t=\int_0^t dt'[K_x^{(+)}(t,t')+K_x^{(-)}(t,t')\langle\sigma_z\rangle_{t'}]. \tag{3.13}$$

The kernels are again given in the form of expansions involving the modified influence functions. We find

$$K_x^{(\pm)}(t,t')=\sum_{n=1}^{\infty}(-1)^{n-1}\int_{t'}^{t}dt_{2n-1}\cdots \times\int_{t'}^{t_3}dt_2\Delta_{2n-1}(\{t_j\})2^{-n}\sum_{\{\xi_j=\pm1\}}\xi_n\widetilde{F}_n^{(\mp)}C_n^{(\pm)}. \tag{3.14}$$

Finally, it is straightforward to see from Eqs. (3.5) and (3.3) that $\langle\sigma_y\rangle_t$ can be obtained from $\langle\sigma_z\rangle_t$ by differentiation,

$$\langle\sigma_y\rangle_t=-\frac{1}{\Delta(t)}\frac{d\langle\sigma_z\rangle_t}{dt}. \tag{3.15}$$

The equivalence of Eq. (3.3) with (3.11) can be seen from the iterative solution of Eq. (3.11) with the insertion of the series (3.12). Indeed one finds that the ensuing expression for $\langle\sigma_z\rangle_t$ coincides with Eq. (3.3). Following similar lines, the equivalence of Eq. (3.4) with Eq. (3.13) can be shown.

So far, our treatment has been exact for general $\Delta(t)$ and $\varepsilon(t)$. In the following, for simplicity, we consider the transfer matrix element Δ as time independent. In the particular cases, we deal with a static strain ϵ_0 as well as with a time-dependent bias $\varepsilon(t)$ as in Eq. (2.2).

IV. ANALYTIC RESULTS IN VARIOUS LIMITS

A. The noninteracting-blip approximation

In practical calculations, suitable truncations in the series expansions of the kernels must be performed. In certain pa-

rameter regimes, the average blip length is small against the average sojourn length. Under this assumption, which has to be confirmed self-consistently, the blip-blip correlations $\Lambda_{j,k}$ are negligible. Also the sojourn-blip interactions $X_{j,k}$ may be disregarded except those with $k=j-1$. The latter are approximately given by $X_{j,j-1}=Q''(\tau_j)$. This approximation has been termed the noninteracting-blip approximation [4]. In the NIBA, the influence function $\Phi^{(n)}$ is approximated by an expression depending on the blip lengths $\{\tau_j\}$ alone,

$$\Phi^{(n)}_{\rm NIBA}=\sum_{j=1}^{n}\,[Q'(\tau_j)-i\xi_j\eta_{j-1}Q''(\tau_j)].$$

Because interblip correlations are disregarded in $\Phi^{(n)}_{\rm NIBA}$, the modified influence factors $\tilde{F}^{(\pm)}_n$ are zero for $n\neq 1$, and the expressions (3.12) and (3.14) are truncated to

$$K_z^{(+)}(t,t')=\Delta^2 e^{-Q'(t-t')}\cos[Q''(t-t')]\cos\vartheta(t,t'),$$

$$K_z^{(-)}(t,t')=\Delta^2 e^{-Q'(t-t')}\sin[Q''(t-t')]\sin\vartheta(t,t'),$$

and

$$K_x^{(+)}(t,t')=\Delta e^{-Q'(t-t')}\sin[Q''(t-t')]\cos\vartheta(t,t'),$$

$$K_x^{(-)}(t,t')=\Delta e^{-Q'(t-t')}\cos[Q''(t-t')]\sin\vartheta(t,t').$$

Evaluation of Eq. (3.11) and of the relations (3.13) and (3.15) with these kernels gives the evolution of the damped TSS within the NIBA. Note that the deterministic forces are fully taken into account. The dynamics of $\langle\sigma_z\rangle_t$ for time-periodic driving has been studied in Refs. [10–13,18]. The regimes in which the NIBA is valid have been discussed in Refs. [4,6] for a static bias, and in Refs. [10,13] for the driven case. Quite generally one has found that the NIBA describes the dynamics of $\langle\sigma_z\rangle_t$ fairly well for high enough temperatures and/or strong enough damping. Indeed, this is confirmed numerically (cf. Fig. 2). In this parameter regime and in the absence of driving, the NIBA correctly predicts either damped oscillations or monotonous relaxation towards the equilibrium values $\langle\sigma_x\rangle_\infty=(\Delta/\epsilon_0)\tanh(\epsilon_0/2T)$ and $\langle\sigma_z\rangle_\infty=\tanh(\epsilon_0/2T)$. When $T\to 0$, this implies $\langle\sigma_x\rangle_\infty\to\Delta/|\epsilon_0|$ and $|\langle\sigma_z\rangle_\infty|\to 1$. This shows unphysical divergence of the coherence for $\epsilon_0\to 0$ and trapping of the population in the lower well for arbitrarily small ϵ_0. Hence, the NIBA becomes unreliable in this regime (cf. Figs. 3–5). This supports the relevance of interblip correlations at low T.

B. Markov limit

In the remainder of this section, we deal with the important case of weak damping $\alpha\ll 1$ for which the coherent regime extends over a broad temperature range. In this subsection, we investigate the high-temperature regime in the so-called Markov limit.

For the Ohmic form (2.4), the force correlation function (2.3) becomes δ correlated for high T and large ω_c,

$$\mathrm{Re}\langle\zeta(t)\zeta(0)\rangle_T=4\alpha\pi T\delta(t), \tag{4.1}$$

which is the Markov limit. Now, $Q(\tau)$ takes the form

$$Q(\tau)=2\alpha\ln(\omega_c/2\pi T)+2\pi\alpha T|\tau|+i\pi\alpha\,\mathrm{sgn}(\tau), \tag{4.2}$$

in which the first term is an integration constant chosen such that Eq. (3.10) smoothly maps on Eq. (4.2) at high T. By this term, the bare tunneling frequency Δ is dressed into the temperature-dependent effective frequency

$$\delta=\Delta(2\pi T/\omega_c)^\alpha=\Delta_r(2\pi T/\Delta_r)^\alpha. \tag{4.3}$$

In the second form, we have introduced the renormalized tunneling matrix element [4]

$$\Delta_r=\Delta(\Delta/\omega_c)^{\alpha/(1-\alpha)}. \tag{4.4}$$

For the form (4.2), the interactions in $\Lambda_{j,k}$ cancel out so that the NIBA becomes *exact* in the Markov limit. For a static bias, the GME (3.11) and the relation (3.13) may be solved by Laplace transformation and algebraic resolution. Upon inserting the transforms of the kernels,

$$K_z^{(+)}(\lambda)=\delta^2[\lambda+2\pi\alpha T]/[(\lambda+2\pi\alpha T)^2+\epsilon_0^2],$$

$$K_z^{(-)}(\lambda)=\delta^2\pi\alpha\epsilon_0/[(\lambda+2\pi\alpha T)^2+\epsilon_0^2],$$

$$K_x^{(+)}(\lambda)=(\pi\alpha/\Delta)K_z^{(+)}(\lambda),$$

$$K_x^{(-)}(\lambda)=K_z^{(-)}(\lambda)/(\pi\alpha\Delta),$$

we find

$$\langle\sigma_z(\lambda)\rangle=\frac{1}{\lambda}\left(1+\frac{(\pi\alpha\epsilon_0-\lambda-2\pi\alpha T)\,\delta^2}{N(\lambda)}\right), \tag{4.5}$$

$$\langle\sigma_x(\lambda)\rangle=K_x^{(+)}(\lambda)/\lambda+K_x^{(-)}(\lambda)\langle\sigma_z(\lambda)\rangle, \tag{4.6}$$

where

$$N(\lambda)=\lambda[(\lambda+2\pi\alpha T)^2+\epsilon_0^2]+\delta^2(\lambda+2\pi\alpha T). \tag{4.7}$$

From this we see that in the Markov limit the dynamics is completely described by the pole at $\lambda=0$, the residue of which represents the equilibrium value

$$\langle\sigma_z\rangle_\infty=\epsilon_0/2T,\quad \langle\sigma_x\rangle_\infty=\delta^2/2\Delta T, \tag{4.8}$$

and by the three poles given by the zeros of the cubic equation $N(\lambda)=0$. At first sight, it seems that there are additional contributions to $\langle\sigma_x\rangle_t$ because of the poles of $K_x^{(+)}(\lambda)$ and $K_x^{(-)}(\lambda)$. However, it turns out that the residues of the two contributions cancel each other.

The characteristics of the cubic equation $N(\lambda)=0$ are as follows (see also the discussion in Ref. [23]). In the limit $|\epsilon_0|\ll\delta$, the zeros of $N(\lambda)$ consist of a real root, $\lambda=-\gamma_r$, describing a relaxational contribution, and of a complex conjugate pair, $\lambda=-\gamma\pm i\Omega$, up to temperature $T=T_1$, where $T_1=(\delta-\epsilon_0^2/2\delta)/\pi\alpha+O(\epsilon_0^4)$. In the regime $T_1<T<T_2$, where $T_2=\delta^2/4\pi\alpha|\epsilon_0|+|\epsilon_0|/2\pi\alpha+O(|\epsilon_0|^3)$, all three roots are negative real. For $T>T_2$, two of them are again complex conjugate. As $|\epsilon_0|$ is raised, the transition temperatures T_1 and T_2 run towards each other, and they coincide at the critical bias strength $|\epsilon_0|=\delta/2\sqrt{2}$. For any stronger bias, two

of the roots are complex conjugate for all temperatures. We now concentrate on this regime. The Vieta relations for γ_r, γ, and Ω read

$$\gamma_r + 2\gamma = 4\pi\alpha T, \tag{4.9}$$

$$\gamma_r(\gamma^2+\Omega^2) = 2\pi\alpha T\delta^2, \tag{4.10}$$

$$\gamma^2 + 2\gamma\gamma_r + \Omega^2 = 4\pi^2\alpha^2T^2 + \epsilon_0^2 + \delta^2. \tag{4.11}$$

Upon picking up the four simple poles by Laplace contour integration, we obtain

$$\langle\sigma_z\rangle_t = a_1 e^{-\gamma_r t} + \langle\sigma_z\rangle_\infty + [(1-a_1-\langle\sigma_z\rangle_\infty)\cos\Omega t + a_2\sin\Omega t]e^{-\gamma t} \tag{4.12}$$

with the amplitudes

$$a_1 = [\Omega^2+\gamma^2-\delta^2-(\Omega^2+\gamma^2)\langle\sigma_z\rangle_\infty]/D, \tag{4.13}$$

$$a_2 = [(\gamma_r-\gamma)a_1 + \gamma(1-\langle\sigma_z\rangle_\infty)]/\Omega,$$

where $D=\Omega^2+(\gamma-\gamma_r)^2$. Similarly, we have

$$\langle\sigma_x\rangle_t = b_1 e^{-\gamma_r t} + \langle\sigma_x\rangle_\infty - [(b_1+\langle\sigma_x\rangle_\infty)\cos\Omega t - b_2\sin\Omega t]e^{-\gamma t}. \tag{4.14}$$

The amplitudes b_1 and b_2 are given by

$$b_1 = [\epsilon_0\delta^2/\Delta - (\Omega^2+\gamma_r^2/4)\langle\sigma_x\rangle_\infty]/D, \tag{4.15}$$

$$b_2 = [\pi\alpha\delta^2/\Delta + (\gamma_r-\gamma)b_1 - \gamma\langle\sigma_x\rangle_\infty]/\Omega.$$

The formulas (4.12)–(4.15) are the exact dynamical expressions for $\alpha \ll 1$ in the Markov regime T above T_0, where T_0 is of the order of Δ_r. These expressions are nonperturbative in the damping strength.

C. Weak damping and low temperatures

In the regime $\alpha \ll 1$ and $T < T_0$, the Markov assumption is not valid. At such low temperatures, even the noninteracting-blip assumption breaks down for weak damping. This is because the kernels $K_z^{(\pm)}$ and $K_x^{(\pm)}$ may receive already in linear order in α contributions from all orders in Δ. On the other hand, in the NIBA only the lowest order in Δ is kept. For zero bias and weak damping, terms of higher order in Δ contribute to the kernel $K_x^{(+)}$, while not to $K_z^{(+)}$. For nonzero bias and weak damping, the NIBA approximation is inconsistent for both kernels $K_x^{(\pm)}$ and $K_z^{(\pm)}$. From this we infer that the NIBA does not describe properly the dynamics of $\langle\sigma_x\rangle_t$ for $T<T_0$ and zero bias. For nonzero bias, low T, and weak damping, also the dynamics of $\langle\sigma_z\rangle_t$ is not treated properly by the NIBA. This is confirmed below.

Consider now systematically the regime of weak damping and low T. To be general, we assume the power-law form $J(\omega)\propto\omega^s$ at low frequencies. It is convenient to absorb the leading cutoff dependence of $Q(\tau)$ in a Franck-Condon factor that renormalizes the bare tunneling matrix. The renormalized frequency scale is

$$\Delta_r^2 = \Delta^2 e^{-q}. \tag{4.16}$$

For super-Ohmic damping ($s>1$), we have

$$q = \frac{1}{\pi}\int_0^\infty d\omega J(\omega)/\omega^2. \tag{4.17}$$

For Ohmic damping ($s=1$), this integral is infrared divergent. It is regularized with a lower cutoff frequency, which is self-consistently identified with Δ_r [4,6], yielding to leading order the renormalized tunneling matrix element (4.4). Keeping q in the exponent for weak damping is important when the cutoff frequency ω_c is very large.

Interestingly enough, the series expressions of the kernels can be summed in linear order of $Q(\tau)$. Following the lines sketched in Refs. [14,25], the z kernels in the weak-damping limit are found to read

$$\begin{aligned} K_z^{(+)}(t,t') = {} & \Delta_r^2\cos\vartheta(t,t')[1+q-Q'(t-t')] \\ & + \Delta_r^4\int_{t'}^t dt_2\int_{t'}^{t_2} dt_1 \sin\vartheta(t,t_2) \\ & \times\langle\sigma_z\rangle_{t_2,t_1}^{(0)}\sin\vartheta(t_1,t')[Q'(t-t')+Q'(t_2-t_1) \\ & - Q'(t_2-t')-Q'(t-t_1)], \end{aligned} \tag{4.18}$$

$$\begin{aligned} K_z^{(-)}(t,t') = {} & \Delta_r^2\sin\vartheta(t,t')Q''(t-t') \\ & - \Delta_r^4\int_{t'}^t dt_2\int_{t'}^{t_2} dt_1 \sin\vartheta(t,t_2) \\ & \times\langle\sigma_z\rangle_{t_2,t_1}^{(0)}\cos\vartheta(t_1,t')[Q''(t-t') \\ & - Q''(t_2-t')]. \end{aligned} \tag{4.19}$$

In these forms, the first terms represent the NIBA. The respective residual term describes a double-blip contribution, which is decorated at the sojourn interval t_2-t_1 in between with $\langle\sigma_z\rangle_{t_2,t_1}^{(0)}$. This insertion accounts for all possible intermediate tunneling events being uninfluenced by the environment. Indeed for weak damping, we may drop the bath correlations in the insertions. Nevertheless, we use Δ_r instead of Δ in view of the possibility that ω_c is very large. Thus we have

$$\langle\sigma_z\rangle_{t,t_0}^{(0)} = \sum_{n=0}^\infty (-\Delta_r^2)^n \int_{t_0}^t \mathcal{D}_{2n}\{t_j\}\prod_{j=1}^n \cos\vartheta(t_{2j},t_{2j-1}).$$

Similarly, the kernels $K_x^{(\pm)}(t,t')$ take the form

$$\begin{aligned} K_x^{(+)}(t,t') = {} & (\Delta_r^2/\Delta)\cos\vartheta(t,t')Q''(t-t') \\ & + (\Delta_r^4/\Delta)\int_{t'}^t dt_2\int_{t'}^{t_2} dt_1\cos\vartheta(t,t_2) \\ & \times\langle\sigma_z\rangle_{t_2,t_1}^{(0)}\cos\vartheta(t_1,t') \\ & \times[Q''(t-t')-Q''(t_2-t')]. \end{aligned} \tag{4.20}$$

$$K_x^{(-)}(t,t') = (\Delta_r^2/\Delta)\sin\vartheta(t,t')[1+q-Q'(t-t')] + (\Delta_r^4/\Delta)\int_{t'}^{t} dt_2 \int_{t'}^{t_2} dt_1 \cos\vartheta(t,t_2) \times \langle\sigma_z\rangle^{(0)}_{t_2,t_1} \sin\vartheta(t_1,t')[Q'(t-t')+Q'(t_2-t_1) - Q'(t_2-t')-Q'(t-t_1)]. \quad (4.21)$$

Consider now first the case in which the driving force $f(t)$ is zero. Then, the insertion at the intermediate sojourn in the expressions (4.18)–(4.21) reads [cf. Eq. (2.6)]

$$\langle\sigma_z\rangle^{(0)}_{t_2,t_1} = \epsilon_0^2/\Omega^2 + (\Delta_r^2/\Omega^2)\cos\Omega(t_2-t_1), \quad (4.22)$$

where $\Omega = (\Delta_r^2+\epsilon_0^2)^{1/2}$. The insertion describes the undamped full dynamics in the interval between a correlated blip pair. Upon interchanging the time integrals in Eqs. (4.18)–(4.21) with the frequency integral defining $Q(\tau)$, the kernels can be calculated in analytic form [25].

The GME (3.11) is solved by Laplace transformation and algebraic resolution. The inversion of the Laplace transformation yields

$$\langle\sigma_z\rangle_t = [\epsilon_0^2/\Omega^2 - \langle\sigma_z\rangle_\infty]e^{-\gamma_r t} + \langle\sigma_z\rangle_\infty + [(\Delta_r^2/\Omega^2)\cos\Omega t + a_2\sin\Omega t]e^{-\gamma t}, \quad (4.23)$$

with amplitude a_2 and equilibrium value $\langle\sigma_z\rangle_\infty$,

$$a_2 = (\gamma_r\epsilon_0^2 + \gamma\Delta_r^2)/\Omega^3 - \gamma_r\langle\sigma_z\rangle_\infty/\Omega, \quad (4.24)$$

$$\langle\sigma_z\rangle_\infty = (\epsilon_0/\Omega)\tanh(\Omega/2T).$$

The incoherent relaxation rate γ_r and the damping rate γ of the oscillatory contribution are given by [25]

$$\gamma_r = (\Delta_r^2/2\Omega^2)J(\Omega)\coth(\Omega/2T), \quad (4.25)$$

$$\gamma = \gamma_r/2 + 2\pi\alpha\delta_{s,1}(\epsilon_0^2/\Omega^2)T,$$

which reduce in the Ohmic case to

$$\gamma_r = \pi\alpha(\Delta_r^2/\Omega)\coth(\Omega/2T),$$

$$\gamma = \gamma_r/2 + 2\pi\alpha(\epsilon_0^2/\Omega^2)T. \quad (4.26)$$

These expressions are exact for weak Ohmic ($s=1$) and weak super-Ohmic ($s>1$) damping. For sub-Ohmic damping ($s<1$), there is no consistent weak damping limit of the form discussed here [14]. According to Eq. (3.15), the quantity $\langle\sigma_y\rangle_t$ is obtained by differentiation of Eq. (4.23).

The dynamics of $\langle\sigma_x\rangle_t$ results from Eq. (3.13) by use of Eq. (4.23) and of the kernels (4.20) and (4.21). We find

$$\langle\sigma_x\rangle_t = [\epsilon_0\Delta_r^2/\Delta\Omega^2 - \langle\sigma_x\rangle_\infty]e^{-\gamma_r t} + \langle\sigma_x\rangle_\infty - [(\epsilon_0\Delta_r^2/\Delta\Omega^2)\cos\Omega t - b_2\sin\Omega t]e^{-\gamma t}, \quad (4.27)$$

where

$$b_2 = (\Delta_r^2/\Delta\Omega)[\pi\alpha + \epsilon_0(\gamma_r-\gamma)/\Omega^2] - \gamma_r\langle\sigma_x\rangle_\infty/\Omega.$$

The equilibrium value is

$$\langle\sigma_x\rangle_\infty = (\Delta_r^2/\Delta\Omega)\tanh(\Omega/2T). \quad (4.28)$$

It is important to note that these results for low T smoothly match those of Sec. IV B around $T=\Delta_r$.

For $\alpha \ll 1$, a useful quantity is the linear combination

$$N(t) = (\epsilon_0/\Omega)\langle\sigma_z\rangle_t + (\Delta/\Omega)\langle\sigma_x\rangle_t, \quad (4.29)$$

which describes the difference between the populations of the ground state and the excited state. We get

$$N(t) = \tanh(\Omega/2T)[1-e^{-\gamma_r t}] + (\epsilon_0/\Omega)[e^{-\gamma_r t} + (\gamma_r/\Omega)\sin(\Omega t)e^{-\gamma t}]. \quad (4.30)$$

This describes relaxation from the initial value ϵ_0/Ω to the equilibrium value $\tanh(\Omega/2T)$. There is also a minor contribution in Eq. (4.30) representing a damped oscillation.

Following these lines, the dynamics of $\langle\sigma_z\rangle_t$ under the influence of a monochromatic high-frequency field has been studied in Ref. [14]. Alternative approaches based on second-order perturbation in the TSS-bath coupling have been frequently employed in this parameter regime. In these treatments, the adiabatic renormalization of the bare tunneling matrix element is usually disregarded. For a discussion of $\langle\sigma_z\rangle_t$ and $N(t)$ under monochromatic low-frequency driving, we refer to Ref. [26].

V. THE INTERACTING-BLIP CHAIN APPROXIMATION

In this section, we deal with the random force beyond the NIBA for general α. The treatment of the stochastic force is improved by taking into account, besides the intrablip interactions, the correlations between all nearest-neighbor blips $\Lambda_{j,j-1}$, and the full interactions of the nearest-neighbor sojourn-blip pairs $X_{j,j-1}$.

Diagrammatically, we have a chain of blips in which the nearest-neighbor interblip correlations are fully included. A pictorial description illustrating the contribution of three blips to $\langle\sigma_z\rangle_t$ is sketched in Fig. 1. Because of the pictorial appearance, this approximation has been termed the ''interacting-blip chain approximation'' [21]. In the IBCA, the influence function $\Phi^{(n)}$ is

$$\Phi^{(n)}_{\rm IBCA} = \sum_{j=1}^{n}[S_j - i\xi_j\eta_{j-1}X_{j,j-1}] + \sum_{j=2}^{n}\xi_j\xi_{j-1}\Lambda_{j,j-1}$$

with the full nearest-neighbor sojourn-blip interaction

$$X_{j,j-1} = Q''_{2j,2j-1} + Q''_{2j-1,2j-2} - Q''_{2j,2j-2}.$$

Again, the deterministic biasing force is fully included.

Consider now the dynamics of $\rho_{\sigma,\sigma'}(t)$ in the IBCA. First of all, we introduce the conditional probabilities $R_+(t;\tau)$ and $R_-(t;\tau)$ for the particle that is released from the diagonal state $\eta_0=+1$ at time zero and that hops at time $t-\tau$ into the final off-diagonal state $\xi_f=+1$ and $\xi_f=-1$, respectively,

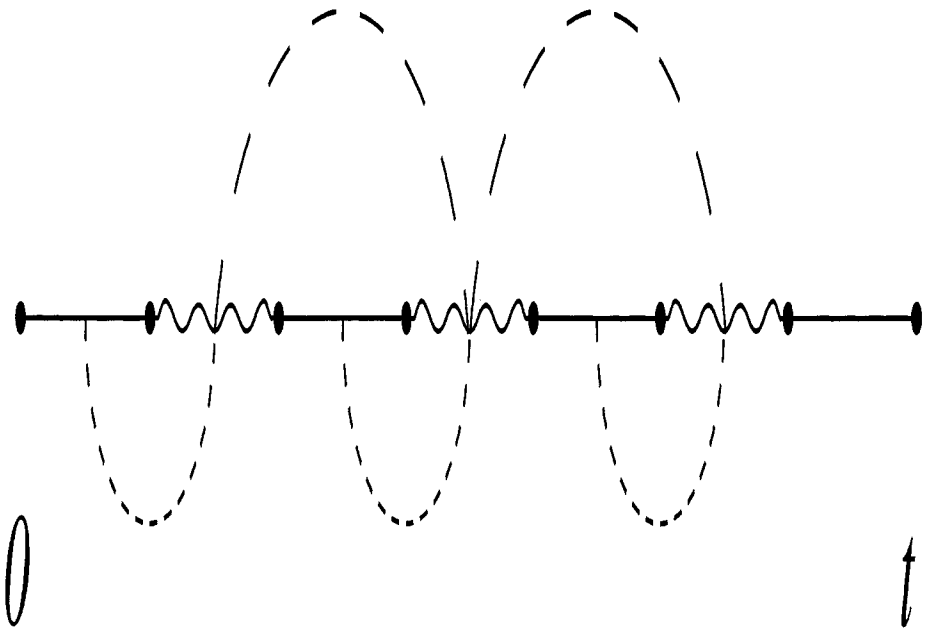

FIG. 1. Three-blip contribution to $\langle\sigma_z\rangle_t$ in the IBCA. The solid line represents a sojourn and the wavy line a blip interval. The blip-blip correlations $\Lambda_{j,j-1}$ are symbolically sketched by a dashed curve and the sojourn-blip correlations $X_{j,j-1}$ by a dotted curve. The intrablip interactions and the individual interactions in $\Lambda_{j,j-1}$ are not displayed.

and afterwards remains there until time t. Shortly, we shall present a set of coupled integral equations for the quantities $R_{\pm}(t;\tau)$.

Upon integrating the conditional probabilities $R_{\pm}(t;\tau)$ over the period τ, one ends up with the off-diagonal elements of the density matrix at time t,

$$\langle\sigma_x\rangle_t=\int_0^t d\tau[R_+(t;\tau)+R_-(t;\tau)], \tag{5.1}$$

$$\langle\sigma_y\rangle_t=i\int_0^t d\tau[R_+(t;\tau)-R_-(t;\tau)]. \tag{5.2}$$

The population $\langle\sigma_z\rangle_t$ ensues from Eq. (5.2) by integration,

$$\langle\sigma_z\rangle_t=1-\Delta\int_0^t dt'\langle\sigma_y\rangle_{t'}, \tag{5.3}$$

as follows from Eq. (3.15). Here, the integration over t' takes into account that the final hop back to the diagonal could be at any time t' in the interval $0\leqslant t'\leqslant t$.

According to Eqs. (5.1)–(5.3), the dynamical problem is solved up to quadratures once the quantities $R_{\pm}(t';\tau)$ are known in the interval $0\leqslant\tau\leqslant t'\leqslant t$.

To derive a set of inhomogeneous coupled integral equations for the conditional probabilities $R_{\pm}(t';\tau)$, we first define a kernel matrix $Y_{\xi,\xi'}(\tau_2,s_1,\tau_1)$ that depends on three time intervals. The kernel matrix represents the possible elementary blip-sojourn-blip processes. It describes a two-step transition from the off-diagonal state ξ', which has been visited for a period τ_1 via an intermediate diagonal state, to the off-diagonal state ξ, which is visited for a period τ_2. The time spent in one of the two intermediate diagonal states is given by s_1. The kernel contains the intrablip interaction of the last blip and the interactions of this blip with the preceding sojourn and with the preceding blip. Performing the sum over the two possible sojourn states in between, the kernel reads

$$Y_{\xi,\xi'}(\tau_2,s_1,\tau_1)=-\xi\xi'\frac{\Delta^2}{2}e^{-Q'(\tau_2)-\xi\xi'\Lambda_{2,1}}\cos X_{21}. \tag{5.4}$$

Next, for a stay in a blip state $\xi=\pm1$, say lasting from time $t'-\tau$ until time t', one has to write a factor

$$B_{\pm}(t',\tau)=\exp\left[\pm i\left(\epsilon_0\tau+\int_{t'-\tau}^{t'}dt''f(t'')\right)\right], \tag{5.5}$$

which takes into account the influences of the deterministic force in the blip in question. In the numerical computation, a major difficulty is that the driving-induced contribution in Eq. (5.5) depends on the absolute times $t'-\tau$ and t' of the blip, and not on the blip length τ alone.

Next, we observe that the factorizing system-reservoir initial state involves that the initial sojourn has infinite length since we put $t_0\to-\infty$. As a result, the initial sojourn-blip pair depends on the blip length τ alone. This special pair is represented by a factor of the form

$$A_{\pm}(\tau)=\mp i(\Delta/2)\exp[-Q'(\tau)\pm iQ''(\tau)]. \tag{5.6}$$

The iteration of the elementary sojourn-blip sequence generates all paths the system can travel. Readily, the sum over all possibilities of stringing together sojourn-blip sequences can be combined in a set of integral equations. Piecing together the elements (5.4)–(5.6), we find

$$R_{\pm}(t';\tau)=B_{\pm}(t',\tau)\Big[A_{\pm}(\tau)+\sum_{k=\pm}\int_0^{t'-\tau}ds \times\int_0^{t'-\tau-s}d\tau' Y_{\pm,k}(\tau,s,\tau') \times R_k(t'-\tau-s;\tau')\Big]. \quad (5.7)$$

The inhomogeneous coupled integral equations (5.7) are the dynamical equations within the IBCA. As remarked before, the dynamics is solved up to quadratures after having computed $R_{\pm}(t';\tau)$ from Eq. (5.7).

A simple numerical algorithm consists in solving Eq. (5.7) by iteration on an equidistant grid in time [21].

The method presented here differs from the iterative solution of the GME (3.11) (cf. Ref. [14]). To include nearest-neighbor blip correlations in the GME, the respective kernel has to be considered at least in order Δ^4. However, iteration of the GME does not lead to linked blip clusters of higher order than considered in the kernel. Furthermore, the GME (3.11) is in the form of a convolution in the absence of time-dependent deterministic forces, while the dynamical equation (5.7) is generally in nonconvolutive form.

As the nearest-neighbor blip correlations constitute the most relevant corrections to the NIBA, the IBCA applies for longer propagation times than the NIBA. The IBCA is most suitable for moderate-to-strong damping. For $\alpha \ll 1$, the treatment given in Sec. IV C is superior.

Systematic improvement of the IBCA is possible along two lines of development. For weak-to-moderate damping, it is suggestive by itself to insert all possible tunneling events of the undamped system into the intervals of the chain links, a proceeding similar to that in Sec. IV C. For higher damping, the first step to do would be to include all next-to-nearest-neighbor interblip correlations. The relevant kernels $Y_{\xi,\xi'}$ would then depend on five time intervals, namely, the lengths of three blips and of two sojourns in between. Upon bookkeeping more and more time intervals in the kernels, the range in which the bath correlations are taken into account exactly is systematically enlarged. The corresponding generalization of the numerical algorithm is clear, but the numerical costs increase drastically with each step.

VI. NUMERICAL SIMULATIONS

In the following, we discuss several illustrative applications of the formulas presented in Secs. IV and V. In contrast to most of the previous works, besides the population $\langle\sigma_z\rangle_t$ we also study the coherences. Because of the simple relation (3.15), the discussion of the quantity $\langle\sigma_y\rangle_t$ is disregarded. We concentrate on four complementary cases. Without exception, we choose Ohmic damping (2.4) with cutoff frequency $\omega_c=30\,\Delta$. In models I and II, the bias is static. In models III and IV, the response to linear and to nonlinear harmonic driving is investigated.

In model I, we choose $T=0.5\Delta$, $\alpha=0.1$, and $\epsilon_0=-0.5\Delta$ for the static bias. This case serves to illustrate that for weak damping the Markov limit is reached already at moderately high temperatures. In Fig. 2, the Markov dynamics as described by the formulas presented in Sec. IV B is compared with the NIBA dynamics based upon the NIBA kernels with the bath correlation function (3.9). The dynamics of $\langle\sigma_z\rangle_t$ and $\langle\sigma_x\rangle_t$ are displayed separately. The dashed curves represent the NIBA while the solid curves describe the Markov limit. Although the temperature is rather low, the underdamped dynamics is fairly well described within the Markov approximation. The minor differences in the asymptotic values originate from the linearization of the tangens hyperbolicus implicit in Eq. (4.8). On the scale of the figures, the curves of the IBCA are very close to the NIBA curves. They are not drawn in Fig. 2. This confirms that interblip correlations are of minor importance in this parameter regime. With increasing T, damping gets larger while the differences between the NIBA and the Markov limit become systematically smaller.

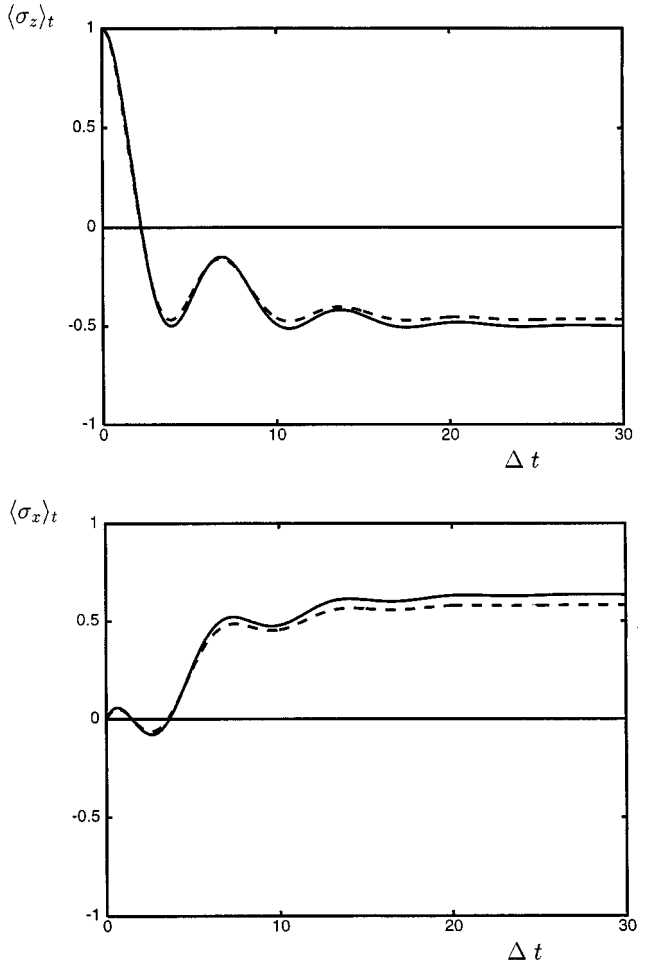

FIG. 2. The population $\langle\sigma_z\rangle_t$ and the coherence $\langle\sigma_x\rangle_t$ are shown for model I ($\alpha=0.1$, $T=0.5\Delta$, $\epsilon_0=-0.5\Delta$). The solid curves represent the Markov limit and the dashed curves the NIBA.

In the remainder, the interest is focused on the dynamics of the TSS at low T, as significant corrections to the NIBA are most likely to occur in this regime. In model II, we choose $T=0.05\Delta, \alpha=0.05$, and zero deterministic bias. In Fig. 3, the coherent dynamics of the population $\langle\sigma_z\rangle_t$ and of the coherence $\langle\sigma_x\rangle_t$ is depicted up to times where the system is almost completely relaxed. The solid curves show the dynamics according to the formulas (4.23) and (4.27). For the population, the NIBA (dashed curve) nearly coincides with the solid curve. The IBCA curve is not displayed since de-

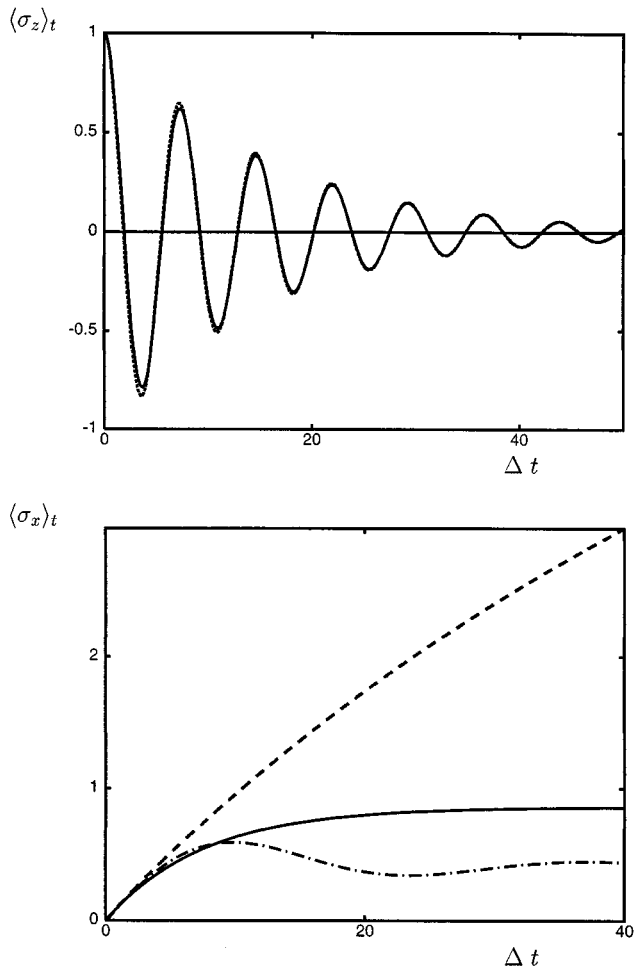

FIG. 3. The population $\langle\sigma_z\rangle_t$ and the coherence $\langle\sigma_x\rangle_t$ are shown for model II ($\alpha=0.05$, $T=0.05\Delta$, $\epsilon_0=0$). The solid curves represent formulas (4.23) and (4.27), and the dashed curves the NIBA. The dash-dotted curve in the plot of $\langle\sigma_x\rangle_t$ represents the IBCA.

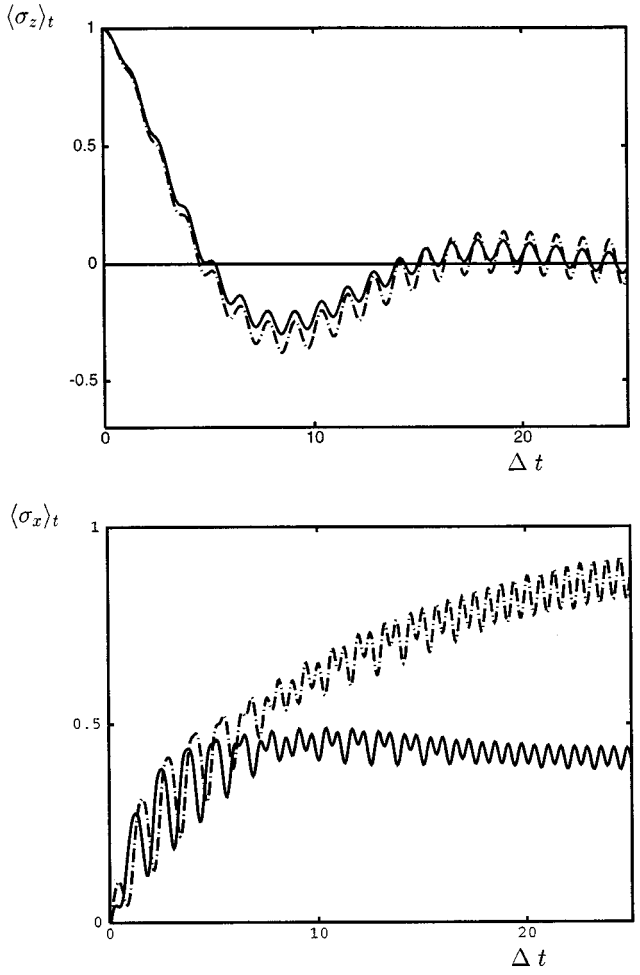

FIG. 4. The population $\langle\sigma_z\rangle_t$ and the coherence $\langle\sigma_x\rangle_t$ are shown for model III ($\alpha=0.25$, $T=0.05\Delta$, $\epsilon_0=0$). The driving force has a moderate amplitude $\epsilon_a=2.5\Delta$, and the frequency ν is 5Δ. The solid curves represent the IBCA and the dash-dotted curves the NIBA. At long times, only *odd* harmonics contribute to $\langle\sigma_z\rangle_t$, and only *even* harmonics to $\langle\sigma_x\rangle_t$.

viations from the other curves are almost undiscernible. From this we see that the leading damping influence in the populations is correctly taken into account by all three methods. The minor deviations are due to the different consideration of higher order terms in the individual approximations.

In contrast, the NIBA (dashed curve) clearly fails for $\langle\sigma_x\rangle_t$. The IBCA (dash-dotted curve) brings about a consistent improvement. The unbounded increase of $\langle\sigma_x\rangle_t$ beyond unity in the NIBA originates from the first term in Eq. (3.13) (the second term does not contribute for zero bias). The time integral over the NIBA kernel $K_x^{(+)}$ increases nearly linearly with t. In the systematic weak-damping treatment, the increase of the integral is eliminated and $\langle\sigma_x\rangle_t$ reaches asymptotically the equilibrium value Eq. (4.28), which is close to one for model II. The full curve represents Eq. (4.27). The IBCA curve describes the dynamics correctly at short times while it overestimates damping at long times. Upon including tunneling events within the intervals of the chain links in Fig. 1, as discussed at the end of Sec. IV C, the modified IBCA coincides with the full curve. In the absence of dissipation, $\langle\sigma_x\rangle_t=0$ for all $t\geqslant 0$ [Eq. (2.6)].

In models III and IV, we choose periodic driving

$$f(t)=\epsilon_a\sin\nu t. \tag{6.1}$$

In model III, we put $T=0.05\Delta$, $\alpha=0.25$, $\nu=5\,\Delta$, and a moderate amplitude $\epsilon_a=2.5\Delta$. We choose $\epsilon_0=0$ in Fig. 4, and $\epsilon_0=-0.5\Delta$ in Fig. 5. The solid curves represent the IBCA and the dash-dotted curves the NIBA.

In Fig. 4, there are again only minor deviations of the IBCA from the NIBA curve for $\langle\sigma_z\rangle_t$, while the differences are drastic for $\langle\sigma_x\rangle_t$. At long times, both the population difference $\langle\sigma_z\rangle_t$ and the coherence $\langle\sigma_x\rangle_t$ reach the time-periodic asymptotic state. For sufficiently strong amplitude ϵ_a, higher order harmonics of the driving frequency become relevant in the asymptotic dynamics. In the absence of a static bias, *selection rules* hold. Namely, only the *odd* harmonics persist at long times in $\langle\sigma_z\rangle_t$, as discussed in Ref. [13]. Following similar lines, upon employing Eqs. (3.11) and (3.13), and observing the symmetry of the kernels under bias inversion, one finds that only the *even* harmonics persist in the asymptotic dynamics of $\langle\sigma_x\rangle_t$ for zero bias. For the moderate driving amplitude ϵ_a chosen in Fig. 4, the fundamental mode governs $\langle\sigma_z\rangle_t$ at long times. It is also visible that $\langle\sigma_x\rangle_t$ asymptotically oscillates with twice the driving frequency. The selection rules for $\epsilon_0=0$ have been confirmed in numerous simulations for different sets of parameters.

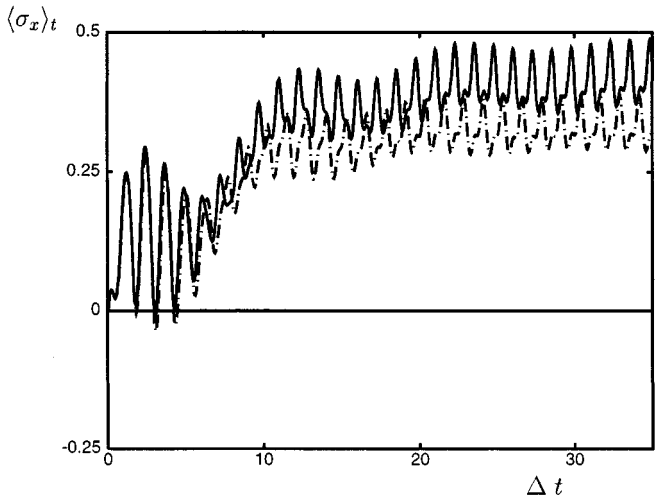

FIG. 5. Plots of $\langle\sigma_x\rangle_t$ for the parameters of model III with additional static bias $\epsilon_0=-0.5\Delta$. For nonzero ϵ_0, also odd harmonics persist at long times.

When a static bias is added, there are again only minor differences between the NIBA and the IBCA curve for $\langle\sigma_z\rangle_t$. For that, the corresponding curves are not shown. For $\langle\sigma_x\rangle_t$, the deviation in the asymptotic dynamics between the IBCA and the NIBA is much smaller as compared with the case $\epsilon_0=0$. However, the deviation is still significant. This indicates that interblip correlations are relevant for $\langle\sigma_x\rangle_t$ in this parameter regime. In Fig. 5, both odd and even harmonics contribute to $\langle\sigma_x\rangle_t$ at long times. This confirms that the above selection rules do not hold when symmetry is broken by a static bias.

Finally, consider model IV in which we choose a symmetric TSS ($\epsilon_0=0$) with $T=0.05\Delta$ and $\alpha=0.25$, as in model III, but with driving frequency $\nu=5\,\Delta$ and amplitude $\epsilon_a=2.4\nu=12\,\Delta$. The parameters are chosen such that the system is dynamically trapped in the initial state in the absence of damping [8] (dash-dotted curve in Fig. 6). This genuine quantum effect is weakened by friction. Nevertheless even for $\alpha=0.25$, the destruction of dynamical localization (DL) still occurs on a much longer time scale than the tunneling period $2\pi/\Delta$ [9] or the relaxation time $1/\gamma_r$ of the undriven TSS (see full curve in Fig. 6). Correspondingly, the coherence $\langle\sigma_x\rangle_t$ oscillates around zero with a small amplitude. In the symmetric TSS considered here, $\langle\sigma_x\rangle_t$ is identified with the difference between the populations of the ground state and of the excited state. Hence, even in the presence of DL in $\langle\sigma_z\rangle_t$, there is a periodic transfer of population between the lower and upper energy eigenstate of the isolated TSS. These findings for the driven TSS should be compared with those for $\epsilon_a=0$. In the absence of driving, the coherence reaches asymptotically a value near $1/2$ (full curve), implying that mainly the ground state is occupied at long times. The differences between the NIBA and the IBCA are minor for $\epsilon_a=12\,\Delta$.

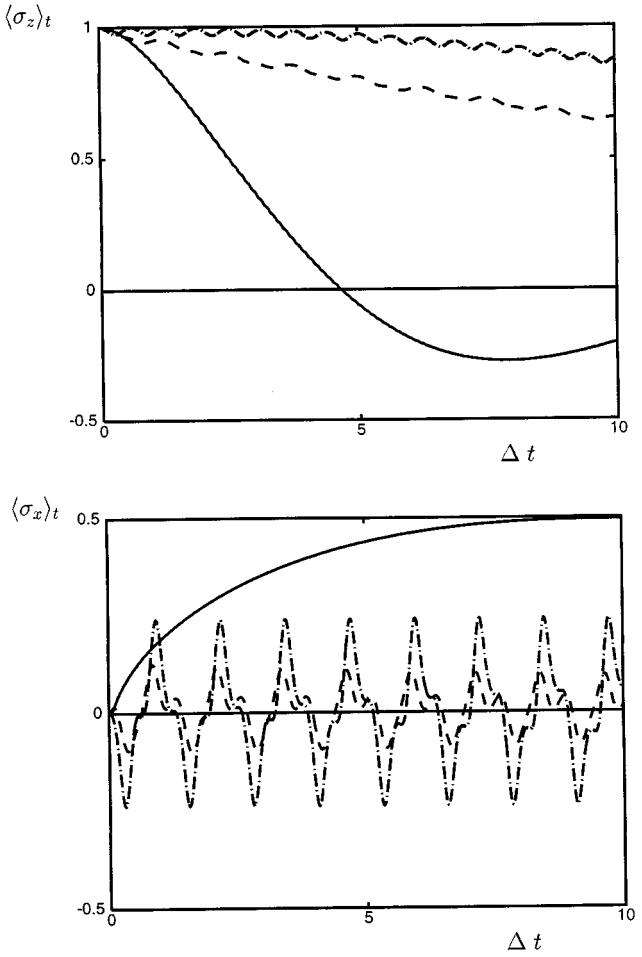

FIG. 6. Plots of $\langle\sigma_z\rangle_t$ and $\langle\sigma_x\rangle_t$ for model IV [same as model III, but $\epsilon_a=12\Delta$ and $\nu=5\Delta$ which satisfy the localization criterion for $\alpha=0$ (dash-dotted curves)]. For $\alpha=0.25$, the localization is still stable (dashed curves) on the time scale on which the undriven system is almost relaxed (full curves). The curves of $\langle\sigma_x\rangle_t$ show an oscillatory transfer of population between the energy eigenstates of the undriven, undamped system.

VII. CONCLUSIONS

We have studied the population difference $\langle\sigma_z\rangle_t$ and the coherences $\langle\sigma_x\rangle_t$ and $\langle\sigma_y\rangle_t$ for the damped driven TSS, which contain complete information about the average dynamics of the reduced system. We have shown in Sec. III B that $\langle\sigma_x\rangle_t$ is related to $\langle\sigma_z\rangle_t$ by an integral relation, while $\langle\sigma_y\rangle_t$ follows from $\langle\sigma_z\rangle_t$ by differentiation. We have also presented an exact generalized master equation for $\langle\sigma_z\rangle_t$. The expressions obtained are exact and hold for general external modulation of both the transfer matrix element and the bias energy of the isolated TSS. In Sec. IV, we have discussed different analytical approaches ranging from the high-temperature or Markov limit to the asymptotic low-temperature regime.

In Sec. V, we have put forward an approach in which the correlations induced by the stochastic force are fully taken into account within all nearest-neighbor blip-sojourn-blip sequences. Because the bath-induced correlations decay with time, the nearest-neighbor interactions represent the most important corrections to the widely used noninteracting-blip approximation. From this we infer that for low temperatures the IBCA should render a correct description of the dynamics for lower α than the NIBA. Indeed, this has been confirmed numerically. Nevertheless, at very low T very long-

ranged correlations that are not described properly by the IBCA may become important at long times. We have given lines along which further improvement beyond the IBCA is achieved.

We have numerically compared the dynamics of the various approaches in Sec. VI for numerous sets of parameters. We have discussed examples in which the NIBA gives a fairly good description of the population $\langle \sigma_z \rangle_t$, but fails to describe the coherences. In the absence of a deterministic bias, e.g., the NIBA expression for $\langle \sigma_x \rangle_t$ violates the unitarity bound for low T and even diverges with time, while the IBCA result stays within the unitarity bound for all times. In the presence of deterministic driving, the NIBA solution for $\langle \sigma_x \rangle_t$ heeds the unitarity bound, but the deviations from the IBCA are still significant at low T.

Further, we have found that, for a harmonically modulated force $f(t)$ and zero static bias, selection rules govern the asymptotic dynamics. Namely, at long times, only odd higher harmonics contribute to the oscillatory dynamics of $\langle \sigma_z \rangle_t$, while only even harmonics persist for $\langle \sigma_x \rangle_t$. Finally, we have studied the forced dynamics for a set of parameters of the monochromatic field for which the undamped TSS is ''dynamically'' localized (DL) in one of the eigenstates of σ_z. For weak dissipation, DL is stable on short-time scales, so that the system remains almost trapped in the initial state. Correspondingly, the coherence $\langle \sigma_x \rangle_t$ oscillates around zero with small amplitude. This indicates an oscillatory transfer of population between the lower and upper energy eigenstate.

ACKNOWLEDGMENTS

M.G. is grateful to P. Hänggi and L. Hartmann for useful discussions. M.W. and U.W. benefitted from stimulating discussions with A. Lück and H. Weber-Gottschick. M.G. acknowledges support by the Deutsche Forschungsgemeinschaft (DFG) under Grant No. HA1517/14-1. M.W. and U.W. acknowledge support by the DFG-SFB 382 ''Verfahren und Algorithmen zur Simulation physikalischer Prozesse auf Höchstleistungsrechnern.''

[1] A. Benderskii, D. E. Makarov, and C. A. Wight, Adv. Chem. Phys. **88**, 1 (1994).
[2] D. M. Eigler and E. K. Schweizer, Nature (London) **344**, 524 (1990); A. A. Louis and J. P. Sethna, Phys. Rev. Lett. **74**, 1363 (1995).
[3] S. Han, J. Lapointe, and J. E. Lukens, Phys. Rev. Lett. **66**, 810 (1991).
[4] A. J. Leggett, S. Chakravarty, A. Dorsey, M. P. A. Fisher, A. Garg, and W. Zwerger, Rev. Mod. Phys. **59**, 1 (1987).
[5] D. Chandler, in *Liquids, Freezing and Glass Transition*, edited by D. Levesque *et al.* (Elsevier, Amsterdam, 1991).
[6] U. Weiss, *Quantum Dissipative Systems*, Series in Modern Condensed Matter Physics (World Scientific, Singapore, 1993), Vol. 2.
[7] S. Chakravarty, Phys. Rev. Lett. **49**, 681 (1982); A. J. Bray and M. A. Moore, *ibid.* **49**, 1545 (1982).
[8] F. Grossmann, P. Jung, T. Dittrich, and P. Hänggi, Phys. Rev. Lett. **67**, 516 (1991); J. M. Gomez Llorente and J. Plata, Phys. Rev. A **45**, R6958 (1992).
[9] T. Dittrich, B. Oelschlägel, and P. Hänggi, Europhys. Lett. **22**, 5 (1993).
[10] M. Grifoni, M. Sassetti, J. Stockburger, and U. Weiss, Phys. Rev. E **48**, 3497 (1993).
[11] Yu. Dakhnovskii, Phys. Rev. B **49**, 4649 (1994); Ann. Phys. (N.Y.) **230**, 145 (1994); J. Chem. Phys. **100**, 6492 (1994).
[12] Yu. Dakhnovskii and R. D. Coalson, J. Chem. Phys. **103**, 2908 (1995).
[13] M. Grifoni, M. Sassetti, P. Hänggi, and U. Weiss, Phys. Rev. E **52**, 3596 (1995).
[14] M. Grifoni, M. Sassetti, and U. Weiss, Phys. Rev. E **53**, R2033 (1996).
[15] R. Löfstedt and S. N. Coppersmith, Phys. Rev. Lett. **72**, 1947 (1994); Phys. Rev. E **49**, 4821 (1994).
[16] M. Grifoni and P. Hänggi, Phys. Rev. Lett. **76**, 1611 (1996); Phys. Rev. E **54**, 1390 (1996).
[17] D. E. Makarov and N. Makri, Phys. Rev. B **52**, R2257 (1995).
[18] I. A. Goychuk, E. G. Petrov, and V. May, J. Chem. Phys. **103**, 4937 (1995); Chem. Phys. Lett. **253**, 428 (1996).
[19] M. Grifoni, Phys. Rev. E **54**, R3086 (1996).
[20] D. E. Makarov and N. Makri, Phys. Rev. E **52**, 5863 (1995).
[21] M. Winterstetter and U. Weiss, Chem. Phys. **217**, 155 (1997).
[22] R. P. Feynman and F. L. Vernon, Ann. Phys. (N.Y.) **24**, 118 (1963).
[23] U. Weiss, H. Grabert, and S. Linkwitz, J. Low Temp. Phys. **68**, 213 (1987).
[24] R. Egger and U. Weiss, Z. Phys. B **89**, 97 (1992).
[25] U. Weiss and M. Wollensak, Phys. Rev. Lett. **62**, 1663 (1989); R. Görlich, M. Sassetti, and U. Weiss, Europhys. Lett. **10**, 507 (1989).
[26] D. A. Parshin, Z. Phys. B **91**, 367 (1993); J. Stockburger, M. Grifoni, and M. Sassetti, Phys. Rev. B **51**, 2835 (1995).